Experimental study of the third-order nonlinearity of atomic and molecular gases using 10-μm laser pulses

J. J. Pigeon, S. Ya. Tochitsky, E. C. Welch, and C. Joshi
UCLA, Los Angeles, California 90095, USA

(Received 8 December 2017; published 13 April 2018)

We present measurements of the third-order optical nonlinearity of Kr, Xe, N_2, O_2, and air at a wavelength near 10 μm by using four-wave mixing of ~15-GW/cm^2, 200-ps (full width at half maximum) CO_2 laser pulses. Measurements in molecular gases resulted in an asymmetric four-wave mixing spectrum indicating that the nonlinear response is strongly affected by the delayed, rotational contribution to the effective nonlinear refractive index. Within the uncertainty of our measurements, we have found that the long-wavelength nonlinear refractive indices of these gases are consistent with measurements performed in the near IR.

DOI: 10.1103/PhysRevA.97.043829

I. INTRODUCTION

Measurements of the third-order optical nonlinearity of atomic and molecular gases are necessary to understand high-intensity light-matter interactions. To date, visible and near-IR laser sources have been used to determine how the magnitude of the third-order nonlinearity varies between various atoms and molecules [1] and how the magnitude of the nonlinearity changes as the driving laser wavelength approaches electronic resonance [2–4]. Due to the small values of the nonlinear refractive index, on the order of 10^{-19} cm^2/W in gases, very high-power laser sources are required for measurements of the third-order nonlinearity for the long-wave IR (LWIR) wavelengths from 8 to 14 μm that are far from the electronic resonance. Therefore, in atomic gases and molecular gases these measurements are required to fully map the dispersion of the electronic third-order susceptibility, a topic of great fundamental importance [1].

Various models [5–7] have been put forth to predict the dispersion of the nonresonant third-order nonlinearity. The most widely used scaling law for gases is the so-called Miller's rule that was first developed to predict the dispersion of the second-order nonlinearity in solids [6] and was later extended to predict the dispersion of the third-order nonlinearity [7,8]. This scaling law is derived from a perturbative treatment of the simple anharmonic oscillator and relates the wavelength dependence of the third-order susceptibility, $\chi^{(3)}$, to that of the first-order susceptibility, $\chi^{(1)}$. Although Miller's rule is frequently invoked to calculate the nonlinear refractive index at long wavelengths from measurements made in the near IR, experiments in the range of 0.4–0.7 μm have shown that this model underestimates the dispersion of the third-order susceptibility and thus has limited predictive power [2]. Therefore, accurate knowledge of the optical nonlinearity of gases in the LWIR requires detailed experimental investigation.

Besides the fundamental importance of third-order nonlinearity measurements in atomic and molecular gases, applications such as pulse compression, supercontinuum generation (SC), and high-power laser propagation in the air benefit from accurate measurements of the third-order nonlinear response. Although there is an extensive database of nonlinear refractive indices at visible and near-IR wavelengths, the data in the mid IR and LWIR are limited because of the lack of laser systems that can produce the GW-class peak powers required to elicit a nonlinear response from gases. There is growing interest, however, in developing sources of intense mid-IR light for applications such as SC generation in the molecular fingerprint region [9] and keV x-ray production via high-harmonic generation [10] for which measurements of optical nonlinearities of atomic and molecular gases in this spectral range would prove useful.

There are a variety of techniques that have been used to measure the nonlinear refractive index including third-harmonic generation [11], self-focusing [12], self-phase modulation [13], cross-phase modulation (XPM) [14,15], and four-wave mixing (FWM) [16–18]. Any of these third-order nonlinear optical processes can be used to measure the third-order susceptibility. However, all self-effects are limited in that they are unable to resolve the nonlinear response in the time domain. For atomic gases, this time resolution may be unnecessary since the optical nonlinearity is related to the response of the bound electron that occurs on a time scale that is instantaneous relative to typical ultrafast laser pulse lengths. For molecules, however, the nonlinear response consists of both instantaneous and delayed components that manifest through a combination of electronic and rotational-vibrational motion [19]. For this reason, the magnitude of the molecular nonlinearity varies in time across the duration of the driving laser pulse. Here, pump-probe measurements relying on XPM have proven the most informative since they can be used to map the temporal behavior of the molecular nonlinearity [14,15]. In contrast, all self-effects measure an effective nonlinear response that is the sum of the instantaneous and delayed components. In this case, the magnitude of the effective molecular nonlinearity is found to vary substantially with the laser pulse duration [13–15,20].

The simplest molecular systems are symmetric diatomic molecules. Here N_2 and O_2 are of great practical importance for applications such as supercontinuum generation and laser filamentation in the air. Owing to their symmetry, these molecules are not IR active and thereby respond to laser fields via the Raman process for which the selection rules for the change in the rotational quantum number, J, are $\Delta J = 0$ and $\Delta J = \pm 2$.

The largest molecular nonlinear response is observed for pulse durations much longer than the characteristic rotational time of a few picoseconds at ~1 atm of pressure. For such conditions, the individual molecules align instantaneously with the driving laser pulse and the nonlinear response is dominated by elastic Rayleigh scattering ($\Delta J = 0$) [20]. For pulse durations on the femtosecond to picosecond time scale, a reduced nonlinearity is observed. Here, the molecules are rotationally excited and the nonlinear response is delayed and dominated by inelastic Raman scattering ($\Delta J = \pm 2$) [14,19]. For pulse durations less than ~20 fs, the nonlinearity asymptotes to a purely electronic response and is the smallest in magnitude [14]. Through the use of time-resolved measurement techniques [14,15], the relative contributions of the electronic and molecular response to the optical nonlinearity at near-IR wavelengths are well understood. At longer wavelengths, however, the existence of multiple rotational-vibrational resonances may influence the molecular nonlinearity of gases. Indeed, recent experiments dedicated to laser filamentation in gases using 2–4-μm lasers [21–23] have already shown that nonlinear optics at long wavelengths may differ from that which occurs at near-IR and visible wavelengths.

In this work, we present measurements of the nonlinear refractive indices of the gases Kr, Xe, N_2, O_2, and air near a wavelength of 10 μm that were realized by studying the FWM of intense, dual-frequency CO_2 laser pulses. By comparing the nonlinear refractive indices of these gases with measurements obtained in the near IR we have attained insight into the wavelength scaling of nonresonant electronic and molecular nonlinearities in the infrared. We have observed that, at intensities of $\sim 10^{10}$ W/cm^2, the third-order nonlinearity of these gases at long wavelengths is close to measurements performed in the near IR. The asymmetry of the FWM spectra obtained in N_2, O_2, and the air indicates that the effective nonlinear indices of molecular gases are dominated by the delayed, rotational contribution to the nonlinear response.

II. EXPERIMENTAL METHOD

The method for measuring the nonlinear refractive index is similar to the one described previously [24] and involves measuring the efficiency of sideband production in a nondegenerate, collinear FWM process. A dual-frequency CO_2 laser pulse was used as a pump source. Experiments were carried out using a high-repetition-rate, picosecond, CO_2 laser system that is described in detail elsewhere [25]. This system is able to generate 3–200-ps pulses amplified on one or two lines of the CO_2 laser. For this study, 200-ps pulses with a peak power of 200 MW, comprised of radiation amplified on the 10P(20) (10.59 μm) and 10R(16) (10.27 μm) lines of the CO_2 laser, were used. Figure 1(a) is a diagram depicting the FWM process studied in this experiment, whereby nonlinear mixing of radiation at wavelengths of 10.59 and 10.27 μm resulted in the generation of Stokes and anti-Stokes sidebands at 10.93 and 9.97 μm, respectively.

Figure 1(b) depicts the experimental setup where the laser pulses were focused with a 2.5-m focal-length NaCl lens to peak intensities of ~15 GW/cm^2 inside of a 2-m-long, gas-filled cell. Upon exiting the cell, the beam was sent through a 4-mm-diameter iris that was used to precisely control the

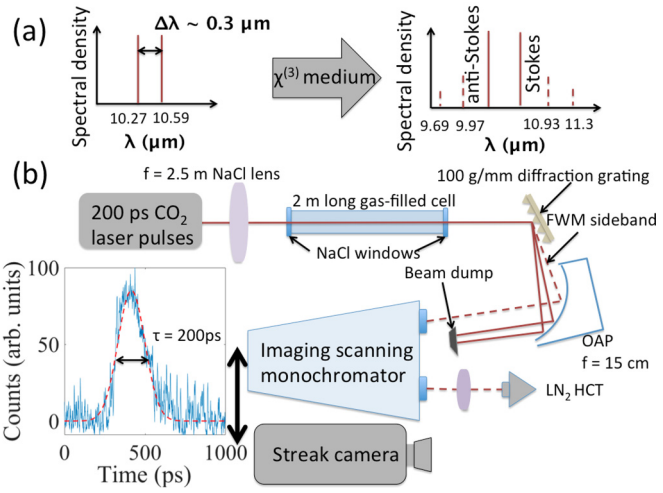

FIG. 1. (a) A dual-wavelength laser pulse is transformed into a family of sidebands by FWM in a nonlinear medium. (b) Experimental setup for nonlinear refractive index measurements of gases. The inset shows a representative temporal pulse profile used for nonlinear refractive index measurements. OAP stands for off-axis parabolic mirror and HCT stands for HgCdTe detector.

area of the analyzed Stokes beam. After the iris, the signal was separated from the pump by reflection from a 150 g/mm diffraction grating. Only the sideband light was then sent through a scanning monochromator to further isolate the signal from the energetic pump. Finally, the energy contained in the sideband was measured using a cryogenic HgCdTe detector. This setup allowed for detection of sideband energies $\sim 10^{-7}$ relative to the pump.

The temporal profile of the pump pulse was measured using a picosecond streak camera with a ~5-ps resolution as shown in Fig. 1(b). Measurements were realized by encoding the temporal pulse profile of the IR pump onto a visible diode laser probe via nonlinear polarization rotation in a CS_2 Kerr cell [26]. This polarization-rotated visible light was then measured using the streak camera. The inset of Fig. 1(b) shows a typical, 200-ps [full width at half maximum (FWHM)] long, temporal pulse profile of the pump laser pulse. The diffraction of the beam was accounted for by measuring the evolution of the spatial beam profile over the 25-cm interaction length using a pyroelectric camera. Figure 2 shows the FWHM beam diameter as a function of distance for the major and minor axes of the elliptical beam used in the experiment. The use of a single focusing optic resulted in an astigmatism of the laser beam that is clearly visible in Fig. 2. The curves presented in Fig. 2 were numerically integrated to calculate the nonlinear refractive indices.

To extract values of the effective nonlinear refractive index we have assumed that the FWM process is perfectly phase matched and that pump depletion is negligible such that the Stokes light varies as [16,17]

$$W_{10.9} = \frac{k_{10.9}^2\, n_{2,\mathrm{eff}}^2\, W_{10.6}^2\, W_{10.3}\, A_{10.9}}{\sqrt{3}\,\tau^2}\left(\int_0^L \frac{dz}{(\pi ab)^{3/2}}\right)^2. \quad (1)$$

In the above, W_λ denotes the energy at each wavelength in microns, $k_{10.9}$ is the vacuum wave number of the Stokes

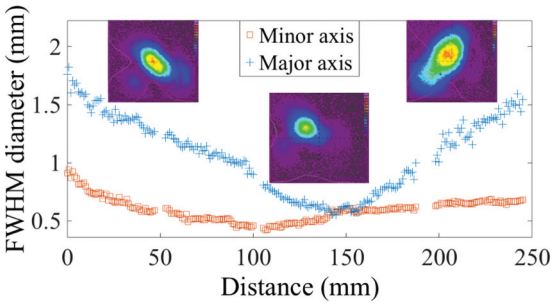

FIG. 2. The evolution of the major and minor diameters of the elliptical beam used for nonlinear refractive index measurements in gases. The insets of the figure show example images of the beam as measured with a pyroelectric camera.

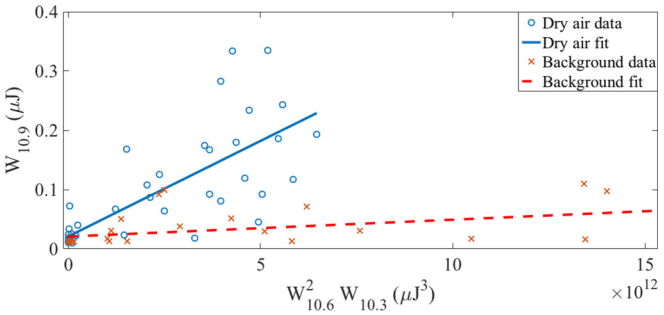

FIG. 4. Energy in the first Stokes sideband plotted as a function of the energy of the 10.6-μm pump times the energy in the 10.3-μm pump squared for 380 Torr of dry air. Note that W_λ is the energy of the laser pulse.

sideband, $n_{2,\mathrm{eff}}$ is the effective nonlinear refractive index, $A_{10.9}$ is the area of the first Stokes beam, and τ is the duration of the laser pulse. The integral of Eq. (1) accounts for the diffraction of the laser beam along the interaction length L. Here a and b are the major and minor axes of the laser beam, respectively. The factor of $\sqrt{3}$ in Eq. (1) arises because the temporal pulse duration of the FWM sideband is $\sqrt{3}$ times shorter than the pump's pulse duration in the low-efficiency limit. According to Eq. (1), the effective nonlinear refractive index can be determined by measuring the slope of the energy produced in the FWM sideband versus the quantity $W^2_{10.6}W_{10.3}$.

The sensitivity of our detection scheme made it necessary to carefully measure the background FWM light produced in IR optics and in transport of the high-power beam through the air. We were unable to use vacuum for background measurements because mirrors within the chamber caused misalignment of the beam at low pressures. Instead, background measurements were carried out by filling the sample cell with an equivalent pressure of He gas having a ∼20× smaller nonlinearity [11] than the gases studied in this work.

At high intensities and fill pressures, avalanche ionization near the focus of the laser beam became an issue. To find a pressure below the threshold of ionization, we first studied the FWM yield as a function of cell pressure in the range of 400–800 Torr. Figure 3 is a plot of the yield of the first anti-Stokes sideband as a function of gas pressure, obtained in

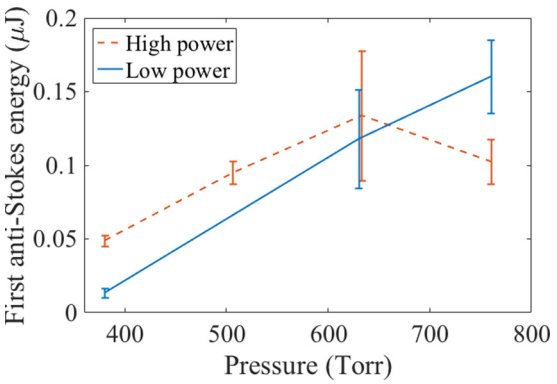

FIG. 3. Energy of the first anti-Stokes sideband as a function of pressure in laboratory air. The dashed and solid lines were produced using 200 and 130 MW, respectively.

laboratory air for powers of ∼200 and 130 MW. Each point on Fig. 3 was obtained by averaging the difference between the FWM signal in the sample cell and the background FWM obtained in the He cell of the same pressure. The error bar on each point of Fig. 3 represents the standard deviation of these averages. Under the assumption that the nonlinear refractive index varies linearly with pressure, the curves in Fig. 3 should be quadratic according to Eq. (1). As can be seen in Fig. 3, this dependence was observed to be linear for the 130 MW (low-power) case and a saturation of the FWM efficiency was observed for the 200 MW (high-power) case. This departure from quadratic scaling was attributed to refraction losses of the FWM sideband due to plasma that resulted in poor collection efficiency at high pressures and laser powers. Consistent with the onset of avalanche ionization, the scattering of the data also increased at high pressures, visible from the error bars presented in Fig. 3.

To avoid issues related to plasma formation we have restricted all quantitative measurements of nonlinear refractive indices to high-purity gases at pressures less than or equal to 380 Torr. Measurements presented for air were made in dry air containing less than 3 ppm of water. Figure 4 shows the FWM yield of the first Stokes sideband as a function of pump energy for 380 Torr of dry air. As can be inferred from the figure, the linear dependence of the sideband energy with respect to the quantity $W^2_{10.6}W_{10.3}$ [see Eq. (1)] suggests that the effect of avalanche ionization, if any, is negligible for this measurement. Figure 4 also shows the dependence of the FWM background as a function of pump energy obtained in 380 Torr of He gas. As can be inferred from Fig. 4, the slope of the line for dry air is larger than that of the background measurement, indicating that the FWM signal generated in dry air is significantly above the FWM background.

To extract the nonlinear refractive indices we have generated plots similar to those presented in Fig. 4 for each gas species under investigation. The nonlinear refractive index for each gas species was then calculated from the difference in the sample and background slope according to Eq. (1). The uncertainty in the nonlinear refractive index measurement was calculated by propagating the uncertainties associated with the measured parameters in Eq. (1). Here we have included the standard deviation of the average pump pulse duration, the uncertainty in the integral of Eq. (1) that accounts for the diffraction of

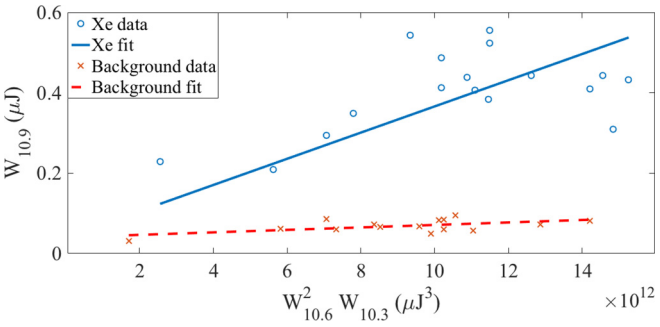

FIG. 5. Energy in the first Stokes sideband plotted as a function of the energy of the 10.6-μm pump squared times the energy in the 10.3-μm pump for 380 Torr of xenon gas. Note that W_λ is the energy of the laser pulse.

the pump beam, and the uncertainty in the least-squares fit used to determine the slope of the FWM yield versus pump energy (see Fig. 4). The latter of these, related to the scattering of the experimental data, was found to dominate the total uncertainty in the nonlinear refractive index measurements. It should be noted that a point-by-point calculation of the nonlinear refractive index from the experimental data was found to produce the same mean value as that calculated from the slope analysis described above.

III. RESULTS AND DISCUSSION

A. Measurements in atomic gases

Let us first consider the nonlinear refractive index data for atomic gases since the nonlinear response in this case is purely electronic. Figure 5 depicts typical FWM data for 380 Torr of Xe gas, where we have plotted the energy in the first Stokes sideband as a function of pump energy. Table I summarizes the extracted nonlinear refractive indices for the noble gases Xe and Kr. It should be noted that we were unable to observe a FWM signal above the noise in Ar. In Table I we have included measurements obtained at 0.8 μm [27] and values for the nonlinear refractive index at 10 μm that have been calculated from the 0.8 μm data using Miller's rule [7].

As can be seen in Table I, the measured nonlinear refractive indices of 5.0×10^{-19} cm^2/W for Xe and 2.9×10^{-19}cm^2/W for Kr are within the experimental uncertainty of measurements made in the near-IR spectral range. The large experimental uncertainties (10%–30%) reported for this work and for similar experiments using high-power, pulsed laser systems make it impossible to detect small deviations from Miller's rule and

TABLE I. Nonlinear refractive indices for noble gases scaled to 1 atm.

Gas species	$\lambda = 0.8\,\mu$m [27] n_2 (10^{-19} cm^2/W)	$\lambda = 10.6\,\mu$m (calculated)[a] n_2(10^{-19} cm^2/W)	$\lambda = 10.6\,\mu$m (measured) n_2(10^{-19} cm^2/W)
Ar	0.97 ± 0.12	0.95 ± 0.12	<1[b]
Kr	2.2 ± 0.4	2.2 ± 0.4	2.9 ± 0.6
Xe	5.8 ± 1.1	5.6 ± 1.1	5.0 ± 1.4

[a]Calculated using Miller's formula [7].
[b]Not measurable in this experiment.

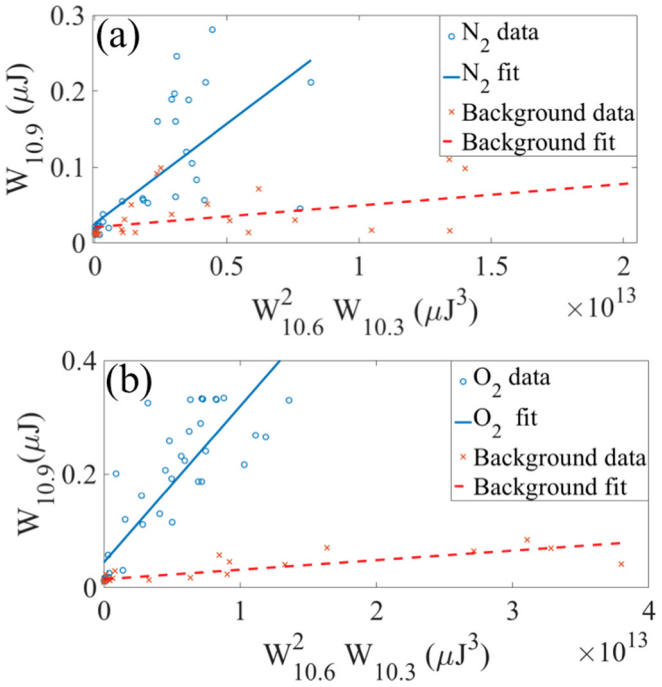

FIG. 6. Energy in the first Stokes sideband plotted as a function of the energy of the 10.6-μm pump times the energy in the 10.3-μm pump squared for (a) 380 Torr of N_2 gas and (b) 250 Torr of O_2 gas. Note that W_λ is the energy of the laser pulse.

other models of the dispersion of the third-order susceptibility. However, our measurements in atomic gases do not contradict the 1%–2% decrease in the nonlinearity predicted using Miller's rule indicating that the scaling law is accurate to within the experimental uncertainty. It should be noted that nonlinearity measurements with experimental uncertainties <2% have been demonstrated [2] and such accurate measurements are necessary for a complete comparison between theory and experiment.

B. Measurements in molecular gases

We now consider our measurements obtained in the diatomic molecules N_2, O_2, and in dry air. Figures 6(a) and 6(b) depict FWM data obtained in 380 Torr of N_2 gas and 250 Torr of O_2 gas, respectively. Here we have plotted the energy in the FWM sideband as a function of pump energy according to Eq. (1). As expected, the difference in the slopes of the sample gas measurement and the He background is the largest for O_2, having an effective nonlinear refractive index more than twice as large as that of N_2 (see Fig. 2). Table II summarizes our measurements for the molecular gases N_2, O_2, and air where these values represent the effective nonlinear refractive index that is the sum of the electronic and molecular response, $n_{2,\mathrm{eff}} = n_{2,\mathrm{elec}} + n_{2,\mathrm{molecular}}$. We have also included nonlinear refractive indices measured at 0.8 [13] and 2.4 μm [15] for comparison with the data obtained in the LWIR. In doing so, we have presented effective nonlinear refractive indices from Refs. [13,15] that were calculated in the long-pulse limit to make a reasonable comparison to our measurements.

As can be inferred from Table II, the nonlinear refractive indices for the molecular gases obtained near 10 μm are in good

TABLE II. Effective nonlinear refractive indices for major air constituents scaled to 1 atm.

Gas species	$\lambda = 0.8\,\mu$m [13] $n_{2,\text{eff}}$ (10^{-19} cm^2/W)	$\lambda = 2.4\,\mu$m [15] $n_{2,\text{eff}}$ (10^{-19} cm^2/W)	$\lambda = 10.6\,\mu$m $n_{2,\text{eff}}$ (10^{-19} cm^2/W)
N_2	3 ± 0.7	3.2 ± 0.5[a]	4.5 ± 0.9
O_2	8 ± 2.2	6.4 ± 0.8[a]	8.4 ± 1.3
Air	4 ± 1.1[b]		5.0 ± 0.9

[a]Calculated from measurements of N_2, O_2, and Ar.
[b]Calculated from measurements in Zahedpour *et al.* using $n_{2,\text{eff}} = n_2 + n_{2,\text{rot}}$ [15].

agreement with those measured at both 0.8- [13] and 2.4-μm [15] wavelengths.

Figure 7 shows a typical FWM spectrum obtained in laboratory air where the amplitude of each sideband was obtained by averaging the difference between the FWM signal obtained in air and that obtained for the He background measurement for ten laser shots of comparable input energy. As seen in Fig. 7, we have observed that conversion to the first Stokes sideband was approximately 5 times as efficient as conversion to the first anti-Stokes sideband. This red asymmetry is consistent with a strong molecular response and is similar to the asymmetry caused by self-phase modulation of 0.8-μm radiation propagating in molecular gases [13]. It should be noted that we did not observe a qualitative difference in the FWM yield between dry air and laboratory air.

The strong molecular response observed in N_2, O_2, and air in the LWIR is likely caused by a number of factors. The use of relatively long, 200-ps pulses certainly acted to induce the strong molecular nonlinearity observed in this experiment. In addition, the use of nondegenerate FWM for nonlinear refractive index measurements may result in a resonant enhancement to the molecular response caused by Raman scattering. We have investigated this by calculating the resonant molecular polarizability of N_2 and O_2 using Eq. (34) of Ref. [1].

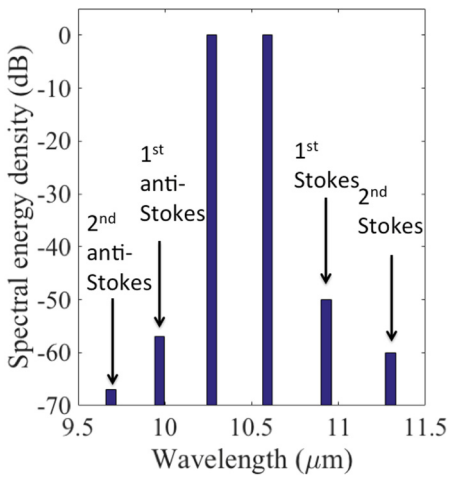

FIG. 7. A typical FWM spectrum obtained in 380 Torr of laboratory air.

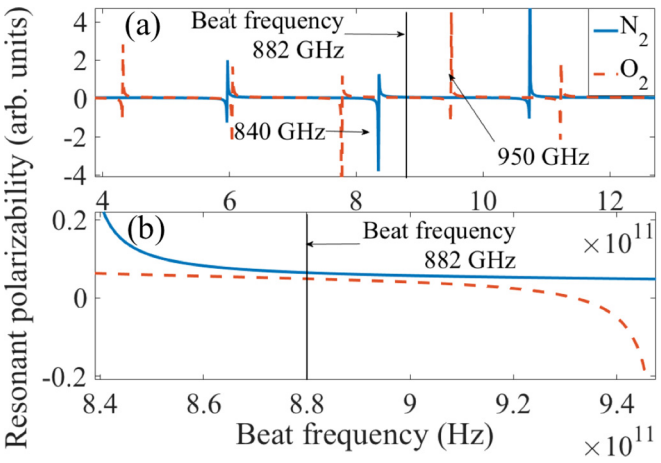

FIG. 8. (a) The resonant third-order polarizability of N_2 and O_2 in the range of 400–1200 GHz and (b) a closeup of the vicinity of the 882-GHz beat frequency used for nonlinear refractive index measurements.

Figure 8(a) is a plot of the resonant polarizability in the range from 400 to 1200 GHz and Fig. 8(b) shows a closeup of the same dependence in the vicinity of the 882-GHz beat frequency used for FWM measurements. Visible on the figure are various rotational Raman transitions of which the $J = 4$ to $J = 2$ transition of N_2 near 840 GHz and the $J = 6$ to $J = 4$ transition of O_2 near 950 GHz are located closest to the 882-GHz beat frequency used for these measurements. However, since the bandwidth of the 200-ps laser pulse and the linewidth of the N_2 and O_2 Raman transitions are both ∼2 GHz, the 40–70-GHz separation may make this resonant enhancement sufficiently small. As a result the effective nonlinear refractive indices presented in Table II are representative of the nonresonant third-order nonlinearity responsible for self-focusing and self-phase modulation. It should be noted that recent experiments on the Kerr self-focusing of ∼1 − TW, 3-ps, 10-μm pulses in air have suggested that the air has an effective nonlinearity close to the value measured in this experiment [28].

IV. CONCLUSIONS

We have presented measurements of the nonlinear refractive index of atomic and molecular gases in the LWIR obtained using collinear FWM of 200-ps CO_2 laser pulses at a wavelength near 10 μm. We have observed that the nonlinear refractive indices of these atomic and molecular gases are close to values measured in the near IR, although high-repetition-rate measurements with small experimental uncertainty are still required to fully test models of the dispersion of the third-order nonlinearity such as Miller's rule. Measurements in molecular gases yielded a strikingly asymmetric FWM spectrum that is indicative of a prominent rotational contribution to the effective nonlinear refractive index for these gases.

Future experiments will be dedicated to nonlinear refractive index measurements in the LWIR range using other methods and laser pulse parameters. For example, nonlinear refractive index measurements relying on third-harmonic radiation generated by 3-ps, 10-μm pulses that are much shorter than the laser pulses used in this study may provide a method

to measure the nonlinearity of atomic and molecular gases at intensities approaching $10^{12}\,\mathrm{W/cm^2}$ while still remaining below the ionization threshold. Finally, the use of shorter pulses or the use of time-resolved measurement techniques may prove valuable in understanding the relative contributions of the electronic and molecular response to the effective nonlinear refractive index of molecules driven by intense LWIR fields.

ACKNOWLEDGMENTS

This material is based upon work supported by the Air Force Office of Scientific Research (AFOSR) under Award No. FA9550-16-1-0139 DEF, the Office of Naval Research (ONR) MURI (Award No. 4-442521-JC-22891), and by the U.S. Department of Energy Grant No. DE-SC001006. We would like to acknowledge Professor Miroslav Kolesik for his thoughtful comments regarding this work.

[1] D. P. Shelton and J. E. Rice, Measurements and calculations of the hyperpolarizabilities of atoms and small molecules in the gas phase, Chem. Rev. **94**, 3 (1994).

[2] V. Mizrahi and D. P. Shelton, Dispersion of Nonlinear Susceptibilities of Ar, N_2, and O_2 Measured and Compared, Phys. Rev. Lett. **55**, 696 (1985).

[3] D. P. Shelton, Nonlinear-optical susceptibilities of gases measured at 1064 and 1319 nm, Phys. Rev. A **42**, 2578 (1990).

[4] M. J. Shaw, C. J. Hooker, and D. C. Wilson, Measurement of the nonlinear refractive index of air and other gases at 248 nm, Opt. Commun. **103**, 153 (1993).

[5] E. L. Dawes, Optical third-harmonic coefficients for the inert gases, Phys. Rev. **169**, 47 (1968).

[6] R. C. Miller, Optical second harmonic generation in piezoelectric crystals, Appl. Phys. Lett. **5**, 1 (1964).

[7] A. Owyoung, Ph.D. thesis, California Institute of Technology, 1972.

[8] W. Ettoumi, Y. Petit, J. Kasparian, and J.-P. Wolf, Generalized Miller formulae, Opt. Express **18**, 7 (2010).

[9] J. J. Pigeon, S. Y. Tochitsky, C. Gong, and C. Joshi, Supercontinuum generation from 2 to 20 μm in GaAs pumped by picosecond CO_2 laser pulses, Opt. Lett. **39**, 11 (2014).

[10] T. Popmintchev, M.-C. Chen, D. Popmintchev, P. Arpin, S. Brown, S. Ališauskas, G. Andriukaitis, T. Balčiunas, O. D. Mücke, A. Pugzlys, A. Baltuška, B. Shim, S. E. Schrauth, A. Gaeta, C. Hernández-García, L. Plaja, A. Becker, A. Jaron-Becker, M. M. Murnane, and H. C. Kapteyn, Bright coherent ultrahigh harmonics in the keV x-ray regime from mid-infrared femtosecond lasers, Science **336**, 1287 (2012).

[11] J. J. Lehmeier, W. Leupacher, and A. Penzkofer, Nonresonant third order hyperpolarizability of rare gases and N_2 determined by third harmonic generation, Opt. Commun. **56**, 67 (1985).

[12] M. Sheik-Bahae, A. A. Said, T. Wei, D. J. Hagan, and E. W. Van Stryland, Sensitive measurement of optical nonlinearities using a single beam, IEEE J. Quantum Electron. **26**, 760 (1990).

[13] E. T. J. Nibbering, G. Grillon, M. A. Franco, B. S. Prade, and A. Mysyrowicz, Determination of the intertial contribution to the nonlinear refractive index of air, N_2, and O_2 by use of unfocused high-intensity femtosecond laser pulses, J. Opt. Soc. Am. B **14**, 650 (1997).

[14] J. K. Wahlstrand, Y. H. Cheng, and H. M. Milchberg, Absolute measurement of the transient optical nonlinearity in N_2, O_2, N_2O, and Ar, Phys. Rev. A **85**, 043820 (2012).

[15] Z. Zahedpour, J. K. Walstrand, and H. M. Milchberg, Measurement of the nonlinear refractive index of air constituents at mid-infrared wavelengths, Opt. Lett. **40**, 5794 (2014).

[16] W. G. Rado, The nonlinear third order dielectric susceptibility of gases and optical third harmonic generation, Appl. Phys. Lett. **11**, 123 (1967).

[17] J. J. Wynne, Optical third-order mixing in GaAs, Ge, Si, and InAs, Phys. Rev. **178**, 1295 (1969).

[18] Y. Kitagawa, R. L. Savage, Jr., and C. Joshi, Demonstration of Collisionally Enhanced Degenerate Four-Wave Mixing in a Plasma, Phys. Rev. Lett. **62**, 151 (1989).

[19] M. Morgen, W. Price, L. Hunziker, P. Ludowise, M. Blackwell, and Y. Chen, Femtosecond Raman-induced polarization spectroscopy studies of rotational coherence in O_2, N_2 and CO_2, Chem. Phys. Lett. **209**, 1 (1993).

[20] D. M. Pennington, M. A. Henesian, and R. W. Hellwarth, Nonlinear index of air at 1.053 μm, Phys. Rev. A **39**, 3003 (1989).

[21] D. Kartashov, S. Ališauskas, A. Pugžlys, A. Voronin, Z. Zheltikov, M. Petrarca, P. Béjot, J. Kasparian, J.-P. Wolf, and A. Baltuška, Mid-infrared laser filamentation in molecular gases, Opt. Lett. **38**, 16 (2013).

[22] A. V. Mitrofanov, A. A. Voronin, D. A. Sidorov-Biryukov, G. Andriukaitis, T. Flöry, A. Pugžlys, A. B. Fedotov, J. M. Mikhailova, V. Ya. Panchenko, A. Baltuška, and A. M. Zheltikov, Post-filament self-trapping of ultrashort laser pulses, Opt. Lett. **39**, 16 (2014).

[23] H. Liang, D. L. Weerawarne, P. Krogen, R. L. Grynko, C.-J. Lai, B. Shim, F. X. Kärtner, and K.-H. Hong, Mid-infrared laser filaments in air at a kilohertz repetition rate, Optica **3**, 7 (2016).

[24] J. J. Pigeon, S. Ya. Tochitsky, E. C. Welch, and C. Joshi, Measurements of the nonlinear refractive index of air, N_2, and O_2 at 10 μm using four-wave mixing, Opt. Lett. **41**, 16 (2016).

[25] S. Ya. Tochitsky, J. J. Pigeon, D. J. Haberberger, C. Gong, and C. Joshi, Amplification of multi-gigawatt 3 ps pulses in an atmospheric CO_2 laser using ac Stark effect, Opt. Express **20**, 13762 (2012).

[26] C. V. Filip, R. Narang, S. Ya. Tochitsky, C. E. Clayton, and C. Joshi, Optical Kerr switching technique for the production of picosecond, multiwavelength CO_2 laser pulse, Appl. Opt. **41**, 3743 (2002).

[27] J. K. Wahlstrand, Y.-H. Cheng, and H. M. Milchberg, High Field Optical Nonlinearity and the Kramers-Kronig Relations, Phys. Rev. Lett. **109**, 113904 (2012).

[28] S. Ya. Tochitsky (private communication).